

Free radical trapping properties of several ethyl-substituted derivatives of 5-ethoxycarbonyl-5-methyl-1-pyrroline *N*-oxide (EMPO)

Klaus Stolze,^{a,*} Natascha Rohr-Udilova,^b Thomas Rosenau,^c
Andreas Hofinger^c and Hans Nohl^a

^a*Molecular Pharmacology and Toxicology Unit, Department of Natural Science,
University of Veterinary Medicine Vienna, Veterinärplatz 1, A-1210 Vienna, Austria*

^b*Institute of Cancer Research, Department of Medicine I, Medical University of Vienna, Borschkegasse 8a, A-1090 Vienna, Austria*

^c*Department of Chemistry, University of Natural Resources and Applied Life Sciences (BOKU),
Muthgasse 18, A-1190 Vienna, Austria*

Received 6 December 2006; revised 6 February 2007; accepted 13 February 2007

Available online 15 February 2007

Abstract—The spin trapping behavior of several ethyl-substituted EMPO derivatives, *cis*- and *trans*-5-ethoxycarbonyl-3-ethyl-5-methyl-pyrroline *N*-oxide (3,5-EEMPO), 5-ethoxycarbonyl-4-ethyl-5-methyl-pyrroline *N*-oxide (4,5-EEMPO), *cis*- and *trans*-5-ethoxycarbonyl-5-ethyl-3-methyl-pyrroline *N*-oxide (5,3-EEMPO), and 5-ethoxycarbonyl-5-ethyl-4-methyl-pyrroline *N*-oxide (5,4-EEMPO), toward a series of different oxygen- and carbon-centered radicals, is described. Considerably different stabilities of the superoxide adducts (ranging from about 12 to 55 min) as well as the formation of other radical adducts were observed.

© 2007 Elsevier Ltd. All rights reserved.

1. Introduction

Previous studies have shown that variation of the substituents in EMPO-derived spin traps has a great influence on the stability of their superoxide spin adducts,^{1–5} especially if a methyl group is present in position 3 or 4 of the pyrroline ring.^{1–3} In the case of 3,5-EDPO (5-ethoxycarbonyl-3,5-dimethyl-pyrroline *N*-oxide) two different diastereomeric forms of the spin trap, which are chemically distinct due to the presence of two symmetric carbon centers in the pyrroline ring, could be separated by conventional column chromatography. The respective *cis*- and *trans*-forms exhibited considerably different spin trapping properties, in contrast to observations made by Tsai et al.⁵ using enantiomers of 5-*t*-butoxycarbonyl-5-methyl-1-pyrroline *N*-oxide. After the addition of superoxide, an additional asymmetric center is created, resulting in the formation of two spectroscopically different spin adducts from either of these compounds. The predominant superoxide spin adduct formed from the

trans-isomer of 3,5-EDPO was found to be very stable ($t_{1/2}$ ca. 45 min), whereas the superoxide adduct from the *cis*-isomer is rather short-lived ($t_{1/2}$ ca. 11 min). The respective stereoisomers from 4,5-EDPO and the other investigated compounds could, however, not be separated into the respective diastereomers using conventional chromatographic procedures. In our attempts to optimize the stability of the spin adducts and also to provide a whole range of spin traps of different lipophilic properties we also investigated a series of pentyl- and phenyl-substituted EMPO derivatives with comparatively poor spin trapping properties.³ In this paper, we describe the spin trapping behavior of several ethyl-substituted EMPO derivatives (*cis*-3,5-EEMPO, *trans*-3,5-EEMPO, *cis*-/*trans*-4,5-EEMPO, *cis*-5,3-EEMPO, *trans*-5,3-EEMPO, and *cis*-/*trans*-5,4-EEMPO) toward a series of different oxygen- and carbon-centered radicals.

2. Results

2.1. Structure of the spin traps

The spin traps synthesized and investigated within the present study can be considered as 5-ethoxycarbonyl-

Keywords: EPR; Spin trapping; Superoxide; EMPO derivatives; Lipid-derived radicals.

* Corresponding author. Tel.: +43 1 25077 4406; fax: +43 1 25077 4490; e-mail: Klaus.Stolze@vu-wien.ac.at

5-methyl-1-pyrroline-*N*-oxide (EMPO) derivatives carrying an ethyl substituent at either C-3, C-4, or C-5. We would like to use the abbreviation EEMPO for these compounds, with two numbers indicating the position of the ethyl substituent and the methyl group, respectively. Thus, 3,5-EEMPO has an ethyl substituent at C-3 and a methyl substituent at C-5 according to the numbering used (see Fig. 1).

Four substitution patterns, 3-ethyl-5-methyl, 4-ethyl-5-methyl, 5-ethyl-3-methyl, and 5-ethyl-4-methyl, were realized. Due to the presence of two stereo centers at C-5 and C-3 (or C-4, respectively) the synthesis afforded a mixture of two diastereomers for each compound with a certain substitution pattern, which in the case of 3,5-EEMPO and 5,3-EEMPO could be separated and purified. Depending on whether the ethoxycarbonyl group and the alkyl substituent at C-3/C-4 are located on the same side of the heterocyclic plane or at different sides, the compounds were designated *cis* or *trans*. The alcohol component of the ester was kept constant as ethyl throughout the current compound series.

The structural identity of the novel spin traps was confirmed by ESI Q-TOF HR-MS (Table 1), FTIR (Table 2), UV-vis, and NMR spectroscopy. A complete set of ^1H , H-H correlated, ^{13}C , HMQC, and HMBC spectra was recorded for each compound, which allowed for a complete signal assignment in both the ^1H and ^{13}C domain. Carbon NMR confirmed the presence of a heterocyclic pyrroline ring. The resonances for C-2 were found around 136–140 ppm according to the respective substitution and configuration pattern, those for C-5 ranged between 79 and 85 ppm. C-5 exhibited a typical down-field shift by about 3 ppm for 5-ethyl substituted compounds as compared to the 5-methyl counterparts. A similar effect of the ethyl group on the shifts of C-4 and C-3 was observed: in compounds without C-4 substituent or with 4-methyl groups resonances were found between 34 and 39 ppm, while the signals for *trans*- and *cis*-4,5-EEMPO (with a 4-ethyl group) appeared at 44.2 and 47.8 ppm, respectively. For the spin traps without 3-substituent or with 3-methyl substitution the C-3 signal appeared at 32–34 ppm, whereas it was down-field shifted to 40.4 and 40.2 ppm for *trans*-3,5-EEMPO and *cis*-3,5-EEMPO, respectively. The shift of the

ethoxycarbonyl group was largely invariant against substitution influences: the carbonyl appeared at about 169–170 ppm throughout, and the ethoxy signals were found at approximately 13.8 and 62.0 ppm.

In contrast to this structure, the resonances of the methyl and ethyl substituents were much more dependent on substitution position and configuration. The 4-methyl substituent was found at 14–15 ppm, the 3-methyl group at 18–19 ppm. The 5a-methyl group was generally found around 21 ppm (with the exception of the *trans*-4,5-EEMPO derivative), where a high-field shift to 14.8 ppm appeared. The methyl resonance of 5-ethyl substituents, being in the range of 7–8 ppm, experienced a down-field shift by 4 ppm for 3-ethyl and 4-ethyl derivatives. The methylene resonances of the ethyl groups were less sensitive to structural changes.

The proton spectra exhibited a typical resonance pattern, too. H-2 exhibited coupling constants of 2.2–2.3 Hz and appeared expectedly as doublet or triplet for 3-substituted and 4-substituted derivatives, respectively. The appearance of H-2 as a triplet—not a doublet of doublets—indicated similar coupling constants to geminal H-3 protons. 3a-CH₃ substituents were found at 1.25 ppm for the *cis*-derivative and at 1.20 ppm for the *trans*-compound, 4a-CH₃ groups resonated more up-field at about 1.18 ppm (*trans*-compound) and 1.09 ppm (*cis*-derivative). The 5a-CH₃ group resonated at 1.58 ppm in 3,5,5-trisubstituted pyrrolines with no difference between *cis*- and *trans*-isomers, whereas in the 4,5,5-trisubstituted counterparts there was an influence of the configuration, with the 5a-CH₃-resonance of the *cis*-isomer (1.70 ppm) being shifted about 0.1 ppm down-field relative to the *trans*-isomer.

Ethyl groups generally showed a diastereotopic splitting of the methylene protons, which was pronounced for 5-ethyl and 4-ethyl groups with two well-separated multiplets and less significant for 3-substituents with the signals of both protons partly overlapping. As an example, in both *cis*- and *trans*-5,3-EEMPO, proton 5a-CH_{2A} appeared as a broad multiplet at 1.92–2.09 ppm and 5a-CH_{2B} as a broad multiplet at 2.18–2.36 ppm.

The signal patterns of the H-3 and H-4 protons exhibited a large dependence on substitution site and configuration, which is in complete agreement with our previous work.^{1–3} In the 4-substituted derivatives the resonance of H-4 gives a good indication of the configuration. The signal of *trans*-derivatives appeared at significantly lower field than that of the *cis*-derivatives: 2.96 ppm versus 2.73 ppm for the 4-methyl derivative and 2.72–2.81 ppm versus 2.22–2.27 ppm for 4-ethyl compounds. The two geminal H-3 protons appeared at about 2.30 ppm/2.90 ppm for the *trans*-compounds and 2.35/2.85 ppm for the *cis*-compounds, the shift differences between the two geminal ring protons being thus slightly larger for the *trans*-isomers. In the *trans*-configured 4-substituted derivatives, the high-field H-4 (about 2.30 ppm) is placed *cis* to the alkyl at C-4 and thus *trans* to the ester. The down-field protons (about 2.90 ppm) are consequently *trans* to the 4-alkyl and thus *cis* to

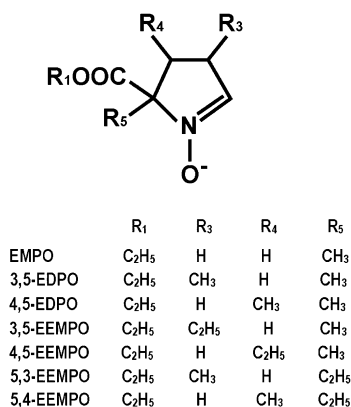


Figure 1. General structure of the spin traps.

Table 1. ESI Q-TOF HR-MS analysis of the spin traps

Sample	Acquired [MH] ⁺	Calcd [MH] ⁺	Error (ppm)	mDa	Acquired [MNa] ⁺	Calcd [MNa] ⁺	Error (ppm)	mDa
<i>cis</i> -3,5-EEMPO	200.1321	200.1283	18.89	3.78	222.1159	222.1108	23.05	5.12
<i>trans</i> -3,5-EEMPO	200.1364	200.1283	40.67	8.14	222.1204	222.1108	43.40	9.64
<i>cis</i> - 4,5-EEMPO	200.1343	200.1283	30.13	6.03	222.1123	222.1108	6.75	1.50
<i>trans</i> - 4,5-EEMPO	200.1421	200.1283	69.06	13.82	222.1134	222.1108	11.62	2.58
<i>cis</i> -5,3-EEMPO	200.1344	200.1283	30.38	6.08	222.1141	222.1108	14.77	3.28
<i>trans</i> -5,3-EEMPO	200.1318	200.1283	17.69	3.54	222.1122	222.1108	6.48	1.44
<i>cis</i> -5,4-EEMPO	200.1389	200.1283	52.77	10.56	222.1172	222.1108	28.81	6.40
<i>trans</i> -5,4-EEMPO	200.1333	200.1283	25.08	5.02	222.1189	222.1108	36.47	8.10

the ester. In the *cis*-4,5-EEMPO derivative, the situation is opposite: the high-field proton (2.35 ppm) is now configured *trans* to 4-alkyl, that is, *cis* to the 5-ethoxy-carbonyl, and the down-field proton (2.85 ppm) *cis* to 4-alkyl, that is, *trans* to the 5-ethoxycarbonyl.

In 3-alkyl-substituted EEMPO derivatives, H-3 appeared at around 3.04 ppm/3.17 ppm for the 3-methyl derivative, and at 2.86 ppm/2.78 ppm for the 3-ethyl counterpart. The shift difference between *cis*- and *trans*-isomers was thus considerably smaller than that of H-4 in 4-alkyl-substituted congeners. The splitting of the geminal H-4 protons was very large for the *trans*-compounds (1.62 ppm vs 2.57 ppm for 3-ethyl and 1.76 ppm vs 2.62 ppm for 3-methyl). In *cis*-configured 3-substituted derivatives, the splitting was significantly smaller (2.11 ppm vs 2.20 ppm for 3-ethyl and 2.07 ppm vs 2.49 ppm for 3-methyl). In the *trans*-derivatives, the high-field protons (1.72 and 1.76 ppm) are configured *cis* to the alkyl groups at C-3 and C-5, and *trans* to the 5-ethoxycarbonyl moiety, the down-field protons (2.57 and 2.62 ppm) *trans* to both alkyl groups and *cis* to the ester. In 3-substituted *cis*-compounds, the situation is again reversed: the high-field protons (2.07 and 2.1 ppm) are now placed *trans* to the two vicinal alkyl groups at C-3 and C-5 (*cis* to the ester), the down-field protons (2.20 and 2.49 ppm) are in *cis*-arrangement to the alkyl groups (*trans* to the ester).

The 1'-methylene groups in the ethoxy moieties of the ester showed pronounced diastereotopic splitting. The resonances were independent of the configuration, and were found around 4.26 ppm for all derivatives with the exception of 3,5-EEMPO (4.12 ppm). Also the methyl resonance in the ethoxy group—generally about 1.30 ppm—was different for the 3,5-EEMPO derivatives (1.17 ppm).

2.2. Spin trapping of superoxide radicals

We tested the spin trapping properties of the EMPO derivatives toward superoxide radicals using an enzymatic system containing hypoxanthine (0.2 mM), xanthine oxidase (50 mU/ml), and the respective spin trap (20 mM) in oxygenated phosphate buffer (20 mM), pH 7.4, containing 0.4 mM DTPA. Immediately after mixing ESR spectra were recorded every 90 s, showing a gradual increase in intensity until an optimal signal intensity was reached about 10 min after mixing. At a later stage only a minor intensity increase was detected and secondary products started to be formed. Therefore,

all spectra shown in Figure 2 were recorded 10 min after mixing. In Figure 2a, the ESR spectrum of the *cis*-3,5-EEMPO superoxide adduct is shown, consisting of two different species. The major species ($a^N = 13.10$ G; $a^H = 7.81$ G; 57%) has very broad lines, possibly indicating either the contribution of unresolved γ -splittings or the presence of two different stereoisomers (rotamers) having only slightly different HFS parameters. The minor species ($a^N = 13.55$ G; $a^H = 15.44$ G; 43%) on the other hand is characterized by very narrow lines. From *trans*-3,5-EEMPO only one adduct was formed (see Table 4). In contrast to 3,5-EEMPO, the respective 4,5-EEMPO could not be separated into the *cis*- and *trans*-forms using conventional chromatographic procedures. When *cis*-/*trans*-4,5-EEMPO was incubated in the hypoxanthine/xanthine oxidase system described above, four different adducts were found in almost equal contribution (Fig. 2b: $a^N = 13.40$ G; $a^H = 9.55$ G; 28% // $a^N = 13.50$ G; $a^H = 11.45$ G; 27% // $a^N = 13.40$ G; $a^H = 6.45$ G; 24% // and $a^N = 13.81$ G; $a^H = 16.33$ G; 21%). From *trans*-5,3-EEMPO (Fig. 2c) and *cis*-/*trans*-5,4-EEMPO (Fig. 2d) two different adducts could be obtained, which were, however, not completely resolved.

In order to determine the half-lives, samples were incubated until maximum intensity was obtained. Then SOD was added and the decay of the signal was recorded as a series of repetitive scans for at least 30 min. In this way the contribution of secondary species could be subtracted from each individual spectrum thus giving more accurate values for the half-lives of the respective superoxide adducts. We also tried solid KO_2 (ca. 1 mg/ml, immediately followed by the addition of SOD and catalase), which resulted in a higher signal-to-noise ratio and a deviation from first order kinetics during the first few minutes (half-life values given in brackets). Despite this fact, the kinetic in the KO_2 system was in good agreement with a first order exponential decay ($r^2 > 0.95$), which was used for calculations of the half-lives (see Table 3). Furthermore, from all 3,5-EEMPO and 5,3-EEMPO isomers, separate half-lives corresponding to the respective *cis*- and *trans*-forms could be obtained. An overview of all relevant parameters is given in Tables 3 and 4.

2.3. Spin trapping of hydroxyl radicals

For the generation of hydroxyl radicals we used a Fenton-type system⁶ consisting of the spin trap (40 mM), hydrogen peroxide (0.2%), EDTA (2 mM), and iron(II) sulfate (1 mM) in water. After 10 s, the reaction

Table 2. IR data (cm^{-1}) of the spin traps

EMPO*	Intensities: strong (1741), medium (1464), weak (950)																			
	2985	2940	2874	1741	1582	1464	1446	1377	1341	1288	1236	1182	1107	1073	1024	950	862	796	—	
<i>c</i> -3,5-EEMPO	2938	2938	2876	1741	1578	1455	1377	1367	1302	1277	1238	1217	1111	1073	1022	942	860	—	674	
<i>t</i> -3,5-EEMPO	2959	2938	2876	1742	1575	1462	1377	1367	1302	1283	1235	1191	1109	1076	1022	—	862	789	670	
4,5-EEMPO	2966	2941	2879	1732	1583	1466	1382	1369	1324	1281	1249	1180	1121	1043	1018	954	862	809	733	
<i>c</i> -5,3-EEMPO	2973	2932	2880	1736	1585	1461	1384	1368	—	1269	1217	—	1138	1105	—	1009	859	—	695	
<i>t</i> -5,3-EEMPO	2974	2938	2880	1739	1581	1456	1385	1368	1273	1227	1202	—	1149	1106	1025	961	857	—	679	
5,4-EEMPO	2976	2941	2882	1738	1580	1461	1387	1367	1274	1256	1240	1178	1137	1120	1098	1005	937	858	772	690

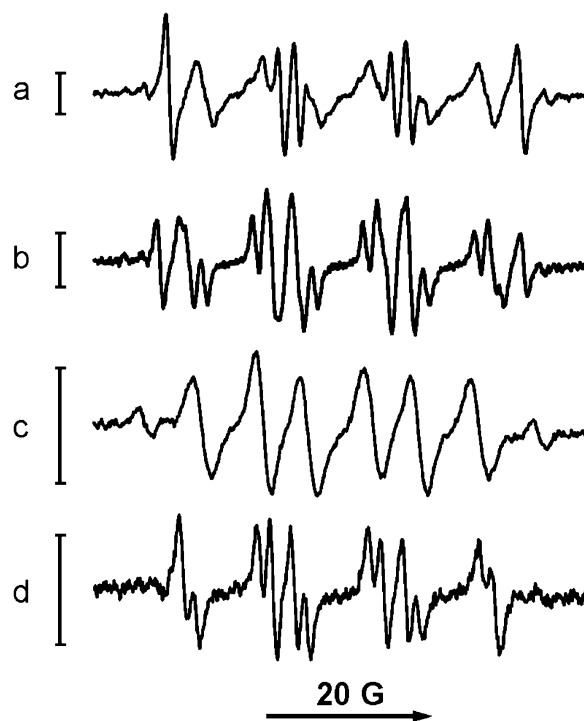
* Data from Stolze et al.¹¹

Figure 2. Formation of the superoxide adducts of the spin traps *cis*-3,5-EEMPO, *cis-trans*-4,5-EEMPO, *trans*-5,3-EEMPO, and *cis-trans*-5,4-EEMPO. (a) *cis*-3,5-EEMPO (20 mM), catalase (250 U/mL), hypoxanthine (0.2 mM), and xanthine oxidase (50 mU/mL) in oxygenated phosphate buffer (20 mM, pH 7.4, containing 0.4 mM DTPA) were incubated and measured using the following EPR parameters: sweep width, 60 G; modulation amplitude, 0.52 G; microwave power, 20 mW; time constant, 0.08 s; receiver gain, 1×10^5 ; scan rate, 42.9 G/min. (b) Same as in (a), except that *cis-trans*-4,5-EEMPO (20 mM) was used. (c) Same as in (a), except that *trans*-5,3-EEMPO (20 mM) was used; sweep width, 80 G; modulation amplitude, 1.05 G; microwave power, 20 mW; time constant, 0.08 s; receiver gain, 5×10^4 ; scan rate, 57.3 G/min. (d) Same as in (a), except that *cis-trans*-5,4-EEMPO (20 mM) was used. The bars represent 5000 arbitrary units.

was stopped upon 1:1 dilution with DTPA (20 mM) in phosphate buffer (300 mM, pH 7.4). In Figure 3a, the hydroxyl radical adduct of *cis*-3,5-EEMPO is shown, consisting of three different species ($a^N = 14.59$ G; $a^H = 19.34$; 70%, $a^N = 13.89$ G; $a^H = 7.94$; 20%, and $a^N = 13.92$ G; $a^H = 6.18$ G, 10%). The respective data obtained from the hydroxyl radical adducts of *cis-trans*-4,5-EEMPO (Fig. 3b), *trans*-5,3-EEMPO (Fig. 3c), and *cis-trans*-5,4-EEMPO (Fig. 3d) are listed in Table 4.

2.4. Spin adducts formed from methanol: methoxyl and hydroxymethyl radical adducts

Methanol was chosen as a model compound for alcohols, from which two different types of radical adducts can be formed: first, the oxygen-centered methoxyl radical adducts (Fig. 4), and second, the carbon-centered hydroxymethyl radical adducts (Fig. 5).

The methoxyl radical adducts were synthesized by nucleophilic addition of methanol using a model system previously described by Dikalov and Mason⁷ and already tested with other spin traps.^{8–11} In Figure 4a, *trans*-

Table 3. Half-life of the superoxide adducts and *n*-octanol/buffer partition coefficients of the spin traps

Compound	Apparent $t_{1/2}$ (min) XOD (KO ₂)	Partition coefficient <i>n</i> -octanol/phosphate buffer (100 mM, pH 7.0)
EMPO*	8.6*	0.15*
<i>cis</i> -3,5-EEMPO	12.32 (10.54)	1.38
<i>trans</i> -3,5-EEMPO	45.09 (33.98)	1.67
<i>cis/trans</i> -4,5-EEMPO	37.07 (33.90)	1.34
<i>cis</i> -5,3-EEMPO	— (22.71)	1.34
<i>trans</i> -5,3-EEMPO	55.04 (30.75)	1.48
<i>cis/trans</i> -5,4-EEMPO	28.09 (34.72)	1.07

* Data from Stolze et al.⁹

3,5-EEMPO/OCH₃ was obtained in a methanolic iron-(III) chloride solution which after 2 min was diluted 1:50 with 300 mM phosphate buffer containing 20 mM DTPA.

cis/trans-4,5-EEMPO/OCH₃ was obtained in the same way (Fig. 4b), but only the *trans*-5,3-EEMPO/CH₂OH adduct could be detected (Fig. 4c) while the expected *trans*-5,3-EEMPO/OCH₃ seemed to be unstable. The *cis/trans*-5,4-EEMPO/OCH₃ adduct is shown in Figure 4d.

For the formation of the hydroxymethyl radical adducts a Fenton-type system⁶ was chosen consisting of the spin trap (40 mM), hydrogen peroxide (0.2%), EDTA (2 mM), and iron-(II) sulfate (1 mM) in methanol/water (20/80, v/v). After 10 s, the reaction was stopped upon 1:1 dilution with DTPA (20 mM) in phosphate buffer (300 mM, pH 7.4). In Figure 5a, the hydroxymethyl radical adduct of *cis*-3,5-EEMPO is shown, consisting of two different species ($a^N = 15.00$ G; $a^H = 24.85$ G; $a^{H(2)} = 0.50$ G; $a^{H(3)} = 0.45$ G; 77%, and $a^N = 14.97$ G; $a^H = 14.00$ G; $a^{H(3)} = 0.56$ G; $a^{H(2)} = 0.30$ G; 23%), which can clearly be distinguished from the methoxyl radical adduct shown above (in Fig. 4a). The respective data obtained from the hydroxymethyl radical adducts of *cis/trans*-4,5-EEMPO (Fig. 5b), *trans*-5,3-EEMPO (Fig. 5c), and *cis/trans*-5,4-EEMPO (Fig. 5d) are listed in Table 4.

2.5. Spin trapping of lipid-derived radicals

Trying to detect lipid-derived free radicals using a recently described Fenton type system^{8,12} containing LOOH instead of hydrogen peroxide mainly resulted in the detection of the hydroxyl radical adduct. We therefore decided to use a UV-irradiated system in toluene previously reported by Clément et al.¹³

In Figure 6a, the radical adduct obtained from *cis*-3,5-EEMPO (50 mM) and excess peroxidized linoleic acid (ca. 100 mM) is shown, consisting of one major species ($a^N = 12.25$ G; $a^H = 14.10$ G). In Figure 6b, the experiment was performed with excess *tert*-butyl hydroperoxide (ca. 300 mM), the spectrum most probably showing the *tert*-butoxyl radical adduct ($a^N = 12.14$ G; $a^H = 13.06$ G; $a^H = 0.62$ G) which decayed rapidly, thereby forming a complicated mixture of secondary products which could not be identified. Similar results

were obtained with *cis/trans*-5,4-EEMPO and peroxidized linoleic acid (Fig. 6c, $a^N = 12.05$ G; $a^H = 7.30$ G; 64%, and $a^N = 12.05$ G; $a^H = 10.30$ G; 36%) or *tert*-butyl hydroperoxide (Fig. 6d, $a^N = 12.15$ G; $a^H = 7.61$ G; 50%, and $a^N = 12.15$ G; $a^H = 10.65$ G; 50%). From the other spin traps no alkoxy radical adducts were obtained. Instead, weak and rather complicated spectra were detected which could, however, not be identified.

3. Discussion

Eight novel EMPO derivatives (four of them as pure *cis*- or *trans*-forms) were synthesized in this study, bearing ethyl substituents in positions 3, 4, or 5, the remaining substituents being a methyl group and a 5-ethoxycarbonyl substituent in all cases. The structure of the compounds was comprehensively characterized by full NMR assignment (¹H and ¹³C), ESI Q-TOF HR-MS, and IR spectroscopy. Determination of the half-lives of the superoxide adducts was done using a first-order exponential decay approximation (Table 3, Pearson correlation coefficient $r^2 > 0.95$). Using a KO₂ system (higher superoxide formation rate) a contribution of second order decay of the superoxide adducts was observed during the first few minutes.

In addition to the half-life of the spin adducts the rate constant of the spin trapping reaction, the spectral line width, the total number of lines, and additional factors, such as enzyme binding or the solubility (aggregate formation) of the spin trap, reduction by antioxidants or buffer constituents, and degradation by transition metal catalyzed reactions (Fenton type reactions, oxidation by Fe³⁺, etc.) play also important roles regarding the overall efficiency of the spin trapping reaction.

In view of these facts the half-life values given in Table 3 are therefore to be interpreted only as a preliminary estimation of the spin trapping performance.

Hydroxyl radical adducts were stable for more than 20 min, whereas the respective methoxyl radical adducts were rather unstable and disappeared within the first 5–10 min (3,5-EEMPO, 4,5-EEMPO, and 5,4-EEMPO) or were not detected at all (from 5,3-EEMPO). From peroxidized linoleic acid lipid-derived radical adducts could be detected in toluene, whereas in aqueous solution the respective hydroxyl radical adducts were the predominant species. Alkoxy radicals undergo rapid β -scission (rate constant ca. 10^6 M⁻¹ s⁻¹) leading to a series of rearranged products^{14–20} and are therefore difficult to detect. On the other hand, UV-irradiation of peroxides in toluene could be used for the detection of both, alkoxy as well as peroxy radical adducts,¹³ depending on the ratio applied between the spin trap and the respective hydroperoxide.

4. Conclusion

In conclusion, four of the eight possible diastereomeric forms of the investigated EEMPO compounds were successfully separated and can be recommended for

Table 4. Comparison of the EPR parameters of different radical adducts of various EEMPO compounds

Radical	HFS (G)	EMPO*		<i>c</i> -3,5-EEMPO		<i>t</i> -3,5-EEMPO		4,5-EEMPO		<i>c</i> -5,3-EEMPO		<i>t</i> -5,3-EEMPO		5,4-EEMPO		<i>t</i> -3,5-EDPO*		4,5-EDPO*			
·OOH		(57%)	(43%)	(57%)	(43%)	(100%)		28%/27%/24%/21%	(50%)	(50%)	(77%)	(23%)	(57%)	(43%)	(100%)	(36%)	(35%)	(29%)			
	<i>a</i> ^N	13.28	13.28	13.10	13.55	13.10		13.40/13.50/13.40/13.81	13.03	13.03	13.03	13.00	13.45	13.46	13.55	13.48	13.48	13.48			
	<i>a</i> ^H	11.89	9.67	7.81	15.44	7.89		9.55/11.45/6.45/16.33	8.26	5.86	7.21	8.79	10.80	8.18	5.98	9.10	11.60	8.55			
	<i>a</i> ^H	—	—	—	—	—		—	—	—	—	—	—	—	—	—	—	1.90			
·OH		(50%)	(50%)	(70%)	(20%)	(10%)	(84%)	(16%)	(71%)	(29%)	(51%)	(49%)	(66%)	(34%)	(64%)	(23%)	(13%)	(67%)	(33%)	(75%)	(25%)
	<i>a</i> ^N	14.00	14.00	14.59	13.89	13.92	13.80	14.26	13.97	14.51	13.80	14.29	13.66	14.11	13.80	13.84	14.17	13.85	14.30	14.00	14.45
	<i>a</i> ^H	15.00	12.58	19.34	7.94	6.18	8.57	18.80	9.04	19.12	9.24	19.28	8.52	19.45	10.81	8.38	19.90	9.00	19.30	10.00	18.60
	<i>a</i> ^H	0.90	—	—	—	0.83	0.93	1.21	—	—	—	—	—	—	—	—	0.75	0.95	1.05	—	
	<i>a</i> ^H	—	—	—	—	0.34 ⁴	0.34 ⁴	0.58	—	—	—	—	—	—	—	—	—	—	—	—	
·H		(100%)		(100%)		(100%)		(100%)	(100%)		(100%)		(100%)		(50%)	(50%)	(100%)		(100%)		
	<i>a</i> ^N	15.52		15.58		15.47		15.63		15.37		15.23		15.37	15.12	15.45		15.57			
	<i>a</i> ^H	22.21		26.16		25.76		26.25		24.88		26.40		26.06	24.14	25.87		25.31			
	<i>a</i> ^H	20.82		16.01		17.72		16.73		17.08		16.57		17.60	18.70	17.50		18.03			
				(0.56)		(0.54)		0.57													
·CH ₃		(100%)		(60%)	(40%)	(90%)	(10%)	(100%)	(52%)	(48%)	(82%)	(18%)	(54%)	(46%)	(89%)	(11%)		(98%)	(2%)		
	<i>a</i> ^N	15.42		15.32	15.45	15.32	15.33	15.43	15.22	15.12	15.02	15.11	14.67	14.80	15.32	15.35		15.40	15.50		
	<i>a</i> ^H	22.30		14.38	26.45	15.23	25.59	17.03	26.56	18.67	15.68	26.19	15.94	22.58	16.74	26.20		18.43	26.73		
	<i>a</i> ^H	—		—	—	—	—	—	—	—	—	—	—	—	—	—		—	—		
·OCH ₃		(50%)	(50%)	(62%)	(38%)	(67%)	(33%)	(57%)	(43%)	(56%)	(44%)	(56%)	(44%)	(56%)	(44%)	(61%)	(39%)	(56%)	(24%)	(20%)	
	<i>a</i> ^N	13.74	13.74	13.61	14.05	13.55	14.00	13.61	13.41	13.73	13.34	13.86	13.51	13.51	13.55	13.95	13.57	13.52	14.13		
	<i>a</i> ^H	10.87	7.81	4.25	16.03	6.26	15.75	8.11	4.09	4.70	14.80	6.39	16.88	5.62	8.88	6.77	16.10	8.55	4.50	16.43	
	<i>a</i> ^H	—	—	1.00	1.05	1.05	1.00	0.87	0.70	0.88	—	0.95	1.05	0.60	0.60	0.99	0.95	0.70	—	—	
·CH ₂ OH		(100%)		(77%)	(23%)	(59%)	(41%)	(71%)	(29%)	(56%)	(44%)	(58%)	(42%)	(100%)		(64%)	(36%)	(98%)	(2%)		
	<i>a</i> ^N	14.95		15.00	14.97	14.76	14.95	15.06	14.97	14.90	14.70	14.74	14.63	14.74		14.73	14.90	15.00	15.00		
	<i>a</i> ^H	21.25		24.85	14.00	16.42	23.83	16.87	18.32	24.83	16.76	24.37	16.74	18.62		17.10	24.33	18.20	25.30		
	<i>a</i> ^H	—		0.45 ³	0.56 ³	0.45 ³	0.50 ²	0.63	0.50 ²	0.50 ²	0.50 ²	0.50 ²	0.50 ²	(0.50) ²							
	<i>a</i> ^H	—		0.50 ²	0.30 ²	—	0.45 ³	0.44	0.34 ²												
·CH(OH)CH ₃		(67%)	(33%)	(100%)		(58%)	(42%)	(63%)	(37%)	(77%)	(23%)	(83%)	(17%)	(100%) ^{**}		(63%)	(37%)	(100%)			
	<i>a</i> ^N	14.94	15.00	14.80		14.80	14.69	15.07	15.05	14.91	14.40	14.66	14.67	14.74		14.84	14.64	15.10			
	<i>a</i> ^H	20.82	22.40	22.76		22.18	16.08	17.63	19.24	23.62	18.96	23.32	16.46	19.12		23.30	17.07	18.46			
·CO ₂ ⁻		(100%)		(100%)		(100%)		(80%)	(20%)	(50%)	(50%)	(50%)	(50%)		(90%)	(10%)	(97%)	(3%)	(95%)	(5%)	
	<i>a</i> ^N	14.74		14.99		14.84		15.30	14.90	14.80	14.67	14.80	14.67		14.87	12.39	14.84	14.84	14.90	14.78	
	<i>a</i> ^H	17.16		14.99		22.74		15.30	23.68	22.63	16.02	22.63	16.02		16.78	12.39	15.55	22.80	15.80	22.70	
	<i>a</i> ^H	—		—		—		—	—	—	—	—	—		1.48	0.38 ⁴	0.30 ⁴	0.35 ⁴	0.30 ⁴		
(LOOH)		(62%)	(38%)	(100%) ^{**}		—		—		—		—	—		(64%)	(36%) ^{**}	(50%)	(45%)	(68%)	(32%)	
	<i>a</i> ^N	13.45	13.45	12.25		—		—		—		—	—		12.05	12.05	14.40	13.75	13.85	14.60	
	<i>a</i> ^H	11.45	8.55	14.10		—		—		—		—	—		7.30	10.30	18.90	8.83	9.90	18.30	
	<i>a</i> ^H	—	—	—		—		—		—		—	—		—	—	—	—	1.05	—	
(<i>t</i> BuOOH)				(100%) ^{**}		—		—		—		—	—		(50%)	(50%) ^{**}					
	<i>a</i> ^N	—		12.14		—		—		—		—	—		12.15	12.15	—	—	—	—	
	<i>a</i> ^H	—		13.06		—		—		—		—	—		7.61	10.65	—	—	—	—	
	<i>a</i> ^H	—		0.62		—		—		—		—	—		—	—	—	—	—	—	

* Data from Stolze et al.²^{**} High line width: unresolved lines.

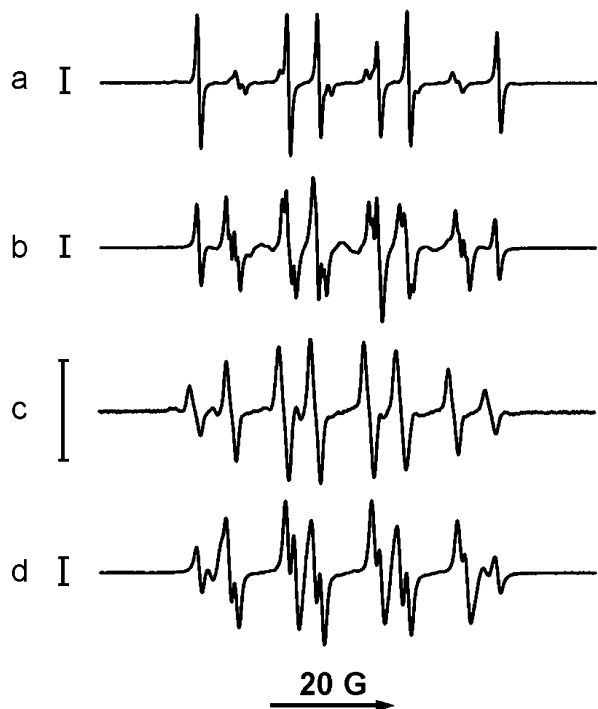


Figure 3. Formation of hydroxyl radical adducts of the spin traps *cis*-3,5-EEMPO, *cis-trans*-4,5-EEMPO, *trans*-5,3-EEMPO, and *cis-trans*-5,4-EEMPO. (a) *cis*-3,5-EEMPO (40 mM) was incubated with a Fenton system containing FeSO_4 (1 mM), EDTA (2 mM), H_2O_2 (0.2%). The reaction was stopped after 10 s by 1:1 dilution with phosphate buffer (300 mM, pH 7.4, containing 20 mM DTPA) and the spectrum was recorded using the following spectrometer settings: sweep width, 80 G; modulation amplitude, 0.23; microwave power, 20 mW; time constant, 0.08 s; receiver gain, 1×10^4 ; scan rate, 57.2 G/min. (b) Same as in (a), except that *cis-trans*-4,5-EEMPO (40 mM) was used. (c) Same as in (a), except that *trans*-5,3-EEMPO (40 mM) was used. (d) Same as in (a), except that *cis-trans*-5,4-EEMPO (40 mM) was used. The bars represent 5000 arbitrary units.

trapping of superoxide radicals when higher lipophilic properties are required. The half-lives of their superoxide adducts are greatly dependent on the stereochemical structure, the highest values being comparable to the respective values observed with the EDPO compounds presented earlier.² Toxicological properties are presently being tested and will be published in the near future. There is no correlation between lipophilicity and the half-life times, but hydrophilic compounds such as DMPO, DEPMPO, EMPO, or *iPr*MPO seem to be less toxic and therefore better suitable for biological studies than the more lipophilic spin traps PBN and 5-*t*-butoxycarbonyl-5-methyl-1-pyrroline *N*-oxide.

5. Experimental

5.1. Chemicals

2-Bromobutanoyl bromide, 2-bromopropionyl bromide, crotonic aldehyde, methacrolein, and *trans*-2-pentenal were purchased from Sigma–Aldrich. Petroleum ether (high boiling, 50–70 °C) was obtained from VWR BDH Prolabo and distilled twice before use. All other chemicals were from Merck.

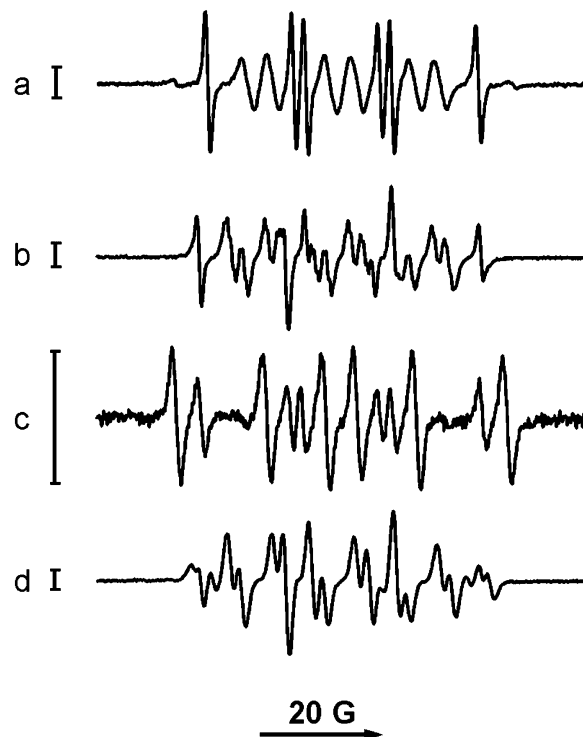


Figure 4. Iron catalyzed addition of methanol to the spin traps *cis*-3,5-EEMPO, *cis-trans*-4,5-EEMPO, *trans*-5,3-EEMPO, and *cis-trans*-5,4-EEMPO. (a) After 2 min incubation of *cis*-3,5-EEMPO (1 M in methanol) with FeCl_3 (2 mM), the reaction was stopped by 1:20 dilution with phosphate buffer (0.15 M, pH 7.4, containing 10 mM DTPA), and the spectrum was recorded with the following spectrometer settings: sweep width, 80 G; modulation amplitude, 0.23 G; microwave power, 20 mW; time constant, 0.08 s; receiver gain, 1×10^4 ; scan rate, 57.2 G/min. (b) Same as in (a), except that *cis-trans*-4,5-EEMPO was used. (c) Same as in (a), except that *trans*-5,3-EEMPO was used. (d) Same as in (a), except that *cis-trans*-5,4-EEMPO was used. The bars represent 1000 arbitrary units.

5.2. Syntheses

Synthesis and characterization of the compounds were performed as reported previously,^{1–3} in analogy to the synthesis of EMPO and its derivatives^{21–23} with minor adaptations as given below.

5.2.1. Ethyl 2-bromobutanoate and ethyl 2-bromopropanoate. 2-Bromobutanoyl bromide (or 2-Bromopropionyl bromide) (70 mmol) was slowly added to a solution of ethanol (100 mmol) and pyridine (70 mmol) in CHCl_3 at 0 °C (ice bath). After stirring for 1 h, the reaction mixture was successively washed with water (50 ml), sulfuric acid (10%, 50 ml), and concentrated aqueous NaHCO_3 (50 ml), and dried over Na_2SO_4 overnight. Solvent and excess ethanol were removed under reduced pressure. The crude, nearly colorless product was used without further purification.

5.2.2. Ethyl 2-nitrobutanoate (or ethyl 2-nitropropanoate). The respective ethyl 2-bromoalkanoate (60 mmol) was added under stirring to a solution of sodium nitrite (7.2 g, 104 mmol) and phloroglucinol dihydrate (8.5 g, 52 mmol) in dry *N,N*-dimethylformamide (120 ml) at

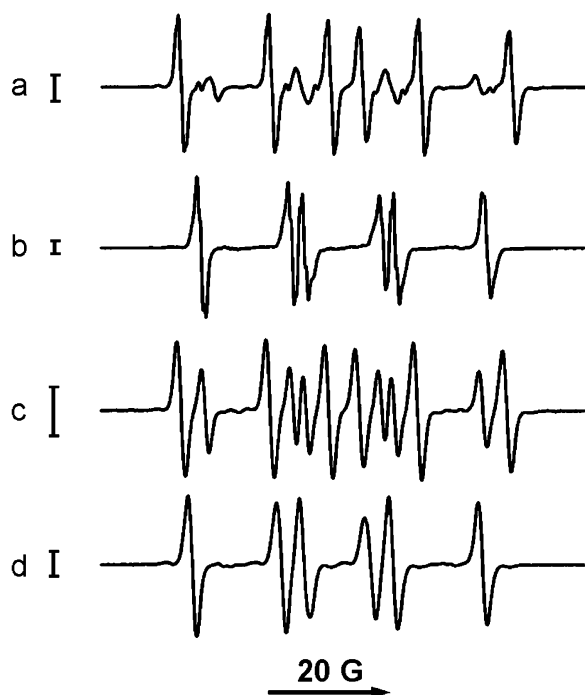


Figure 5. Formation of hydroxymethyl radical adducts of the spin traps *cis*-3,5-EEMPO, *cis*-*trans*-4,5-EEMPO, *trans*-5,3-EEMPO, and *cis*-*trans*-5,4-EEMPO. (a) *cis*-3,5-EEMPO (40 mM) was incubated with Fenton system containing FeSO_4 (1 mM), EDTA (2 mM), H_2O_2 (0.2%) in the presence of 10% methanol. The reaction was stopped after 10 s by 1:1 dilution with phosphate buffer (300 mM, pH 7.4, containing 20 mM DTPA) and the spectrum was recorded using the following spectrometer settings: sweep width, 80 G; modulation amplitude, 0.23 G; microwave power, 20 mW; time constant, 0.08 s; receiver gain, 1×10^4 ; scan rate, 57.2 G/min. (b) Same as in (a), except that *cis*-*trans*-4,5-EEMPO (40 mM) was used. (c) Same as in (a), except that *trans*-5,3-EEMPO (40 mM) was used. (d) Same as in (a), except that *cis*-*trans*-5,4-EEMPO (40 mM) was used. The bars represent 5000 arbitrary units.

room temperature. The solution was stirred overnight, poured into ice water (240 ml), and extracted 4 times with ethyl acetate (100 ml). The combined extracts were treated twice with 100 ml of saturated NaHCO_3 solution and dried over Na_2SO_4 . After removal of the solids by filtration, the solvent was evaporated in vacuo. The obtained colorless or pale yellow products were used without further purification.

5.2.3. Ethyl 2-ethyl-4-formyl-2-nitropentanoate. Ethyl 2-nitrobutanoate (3.7 g, 23 mmol) was dissolved in a mixture of acetonitrile (10 g, 244 mmol) and triethylamine (0.2 g, 2 mmol). Methacrolein (2.66 g, 38 mmol) was slowly added at 0 °C. The solution was kept at 10 °C overnight and then poured into a solution of ice-cold HCl (5 ml of concentrated HCl in 150 ml of water). The solution was extracted 3 times with CH_2Cl_2 and dried over Na_2SO_4 . After filtration, the mixture was distilled under reduced pressure, and the purity of the remaining product was assessed by thin layer chromatography and IR spectroscopy (Table 2).

5.2.4. Ethyl 2-ethyl-4-formyl-3-methyl-2-nitro-butanoate. Same conditions as above, except that crotonic aldehyde

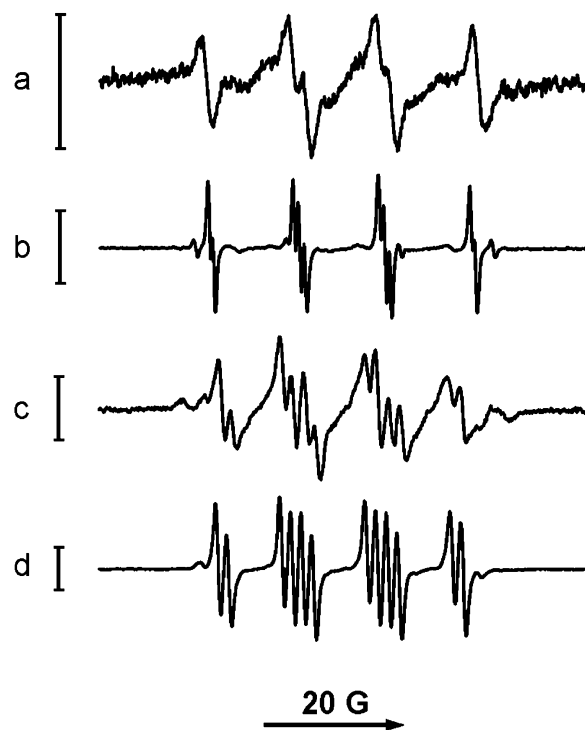


Figure 6. Hydroperoxide-derived free radical adducts of *cis*-3,5-EEMPO and *cis*-*trans*-5,4-EEMPO formed from peroxidized linoleic acid and *tert*-butylhydroperoxide in UV-irradiated toluene solution (a) a nitrogen-bubbled solution of peroxidized linoleic acid (100 mM) and *cis*-3,5-EEMPO (50 mM) in toluene was irradiated for 10 s and the spectrum was recorded with the following spectrometer settings: sweep width, 70 G; modulation amplitude, 0.21 G; microwave power, 10 mW; time constant, 0.04 s; receiver gain, 1×10^5 ; scan rate, 100.2 G/min. (b) A nitrogen-bubbled solution of *tert*-butylhydroperoxide (300 mM) and *cis*-3,5-EEMPO (50 mM) in toluene was irradiated for 10 s and the spectrum was recorded with the following spectrometer settings: sweep width, 70 G; modulation amplitude, 0.1 G; microwave power, 10 mW; time constant, 0.08 s; receiver gain, 1×10^4 ; scan rate, 50.1 G/min. (c) Same as in (a), except that *cis*-*trans*-5,4-EEMPO was used. Spectrometer settings: sweep width, 70 G; modulation amplitude, 0.21 G; microwave power, 10 mW; time constant, 0.02 s; receiver gain, 1×10^5 ; scan rate, 200.3 G/min. (d) Same as in (b), except that *cis*-*trans*-5,4-EEMPO was used. Spectrometer settings: sweep width, 70 G; modulation amplitude, 0.1 G; microwave power, 10 mW; time constant, 0.08 s; receiver gain, 1×10^4 ; scan rate, 50.1 G/min. The bars represent 5000 arbitrary units.

(2.66 g, 38 mmol) was used instead of methacrolein. In addition, the solution had to be stirred for several days at room temperature.

5.2.5. Ethyl 4-formyl-2-methyl-2-nitrohexanoate. Same conditions as above, except that ethyl 2-nitropropanoate (3.4 g, 23 mmol) and ethacrolein (3.2 g, 38 mmol) were used instead of ethyl 2-nitrobutanoate and methacrolein, respectively.

5.2.6. Ethyl 3-ethyl-4-formyl-2-methyl-2-nitrobutanoate. Same conditions as above, except that ethyl 2-nitropropanoate (3.4 g, 23 mmol) and *trans*-2-pentenal (3.2 g, 38 mmol) were used instead of ethyl 2-nitrobutanoate and methacrolein, respectively.

5.2.7. Synthesis of the *N*-oxides. Synthesis of the nitrones was performed according to the procedure described recently for the synthesis of EMPO derivatives.^{1–3,21} To a concentrated solution of 25 mmol of the respective ethyl 2-alkyl-4-formyl-2-nitroalkanoate in H₂O/CH₃OH (v/v = 6:4), an aqueous solution of ammonium chloride (1.87 g in 8 ml of water) was added. While zinc dust (8.5 g, 130 mmol) was slowly added within 30 min, the mixture was carefully kept at room temperature. The mixture was stirred for 4.5 h at room temperature, the white precipitate and the remaining zinc powder were removed by filtration, and the residue was washed five times with methanol (30 ml). The liquid phase was concentrated to about 10 ml, saturated with borax, and extracted 4 times with 60 ml CH₂Cl₂. The organic phase was dried with Na₂SO₄, filtered, and concentrated. Careful purification by column chromatography on silica gel with a petroleum ether/ethanol gradient allowed the separation from the majority of side products and provided the product as a yellow oil or yellow needles. Additional purification was done immediately before the EPR experiments on a 1 ml solid phase extraction column using a Chromabond C-18 100 mg column obtained from Macherey-Nagel (Düren, Germany). The purity of the obtained products was assessed by TLC and UV spectroscopy. Final identification of the purified products was performed by ¹H NMR, ¹³C NMR, ESI Q-TOF HR-MS (Table 1), and IR spectroscopy (Table 2).

5.2.8. NMR. ¹H NMR spectra were recorded at 300.13 MHz, ¹³C NMR spectra at 75.47 MHz with CDCl₃ as the solvent and TMS as the internal standard - if not stated otherwise. Data are given in ppm units. ¹³C peaks were assigned by means of HMQC and HMBC spectra. The numbering of carbons follows the conventions in spin trap studies, it should be noted that the numbering of the heterocyclic atoms runs opposite to conventional heterocycle nomenclature (C-2 is the double-bonded carbon, while C-5 is the quaternary C carrying the ethoxycarbonyl group).

5.2.8.1. *trans*-3,5-EEMPO. ¹H NMR: 0.85 (t, 3H, ^{3b}CH₃), 1.17 (m, 3H, ²CH₃), 1.28–1.54 (m, 2H, ^{3a}CH₂), 1.59 (s, 3H, ^{5a}CH₃), 1.62 (dd, 1H, ⁴CH_B, *trans* to ester, *cis* to Et and Me), 2.57 (dd, 1H, ⁴CH_A, *cis* to ester, *trans* to Et and Me), 2.86 (m, 1H, ³CH), 4.12 (m, 2H, ¹CH₂), 6.82 (d, 1H, ³J = 2.0 Hz, ²CH). ¹³C NMR: 11.4 (^{3b}CH₃), 13.9 (²CH₃), 21.7 (^{5a}CH₃), 26.5 (^{3a}CH₂), 39.2 (⁴CH₂), 40.4 (³CH), 62.2 (O—¹CH₂); 79.4 (⁵C); 139.0 (N=CH), 170.1 (COO).

5.2.8.2. *cis*-3,5-EEMPO. ¹H NMR: 0.85 (t, 3H, ^{3b}CH₃), 1.17 (m, 3H, ²CH₃), 1.28–1.54 (m, 2H, ^{3a}CH₂), 1.58 (s, 3H, ^{5a}CH₃), 2.11 (m, 1H, ⁴CH_B, *cis* to ester), 2.20 (m, 1H, ⁴CH_B, *trans* to ester), 2.78 (m, 1H, ³CH), 4.12 (m, 2H, ¹CH₂), 6.78 (d, 1H, ³J = 2.2 Hz, ²CH). ¹³C NMR: 11.6 (^{3b}CH₃), 14.0 (²CH₃), 21.4 (^{5a}CH₃), 26.4 (^{3a}CH₂), 38.1 (⁴CH₂), 40.2 (³CH), 62.2 (O—¹CH₂); 79.4 (⁵C); 138.0 (N=CH), 169.9 (COO).

5.2.8.3. *trans*-5,3-EEMPO. ¹H NMR: 0.97 (t, 3H, ^{5b}CH₃), 1.20 (d, 3H, ^{3a}CH₃), 1.29 (t, 3H, ²CH₃), 1.76 (dd, 1H, ⁴CH_B, *trans* to ester, *cis* to Et and Me), 1.92–2.09 (m, 1H, ^{5a}CH_{2A}), 2.18–2.36 (m, 1H, ^{5a}CH_{2B}), 2.62 (dd, 1H, ⁴CH_A, *cis* to ester, *trans* to Et and Me), 3.17 (m, 1H, ³CH), 4.26 (m, 2H, ¹CH₂), 6.91 (d, 1H, ³J = 3.6 Hz, ²CH). ¹³C NMR: 7.2 (^{5b}CH₃), 13.9 (²CH₃), 18.4 (^{3a}CH₃), 25.8 (^{5a}CH₂), 33.7 (³CH), 36.4 (⁴CH₂), 62.0 (O—¹CH₂); 83.1 (⁵C); 140.4 (N=CH), 170.1 (COO).

5.2.8.4. *cis*-5,3-EEMPO. ¹H NMR: 0.95 (t, 3H, ^{5b}CH₃), 1.25 (d, 3H, ^{3a}CH₃), 1.31 (t, 3H, ²CH₃), 1.92–2.09 (m, 1H, ^{5a}CH_{2A}), 2.07 (m, 1H, ⁴CH_B, *cis* to ester), 2.18–2.36 (m, 1H, ^{5a}CH_{2B}), 2.49 (dd, 1H, ⁴CH_A, *trans* to ester), 3.04 (m, 1H, ³CH), 4.26 (m, 2H, ¹CH₂), 6.90 (d, 1H, ³J = 2.7 Hz, ²CH). ¹³C NMR: 7.0 (^{5b}CH₃), 13.8 (²CH₃), 19.1 (^{3a}CH₃), 25.2 (^{5a}CH₂), 33.1 (³CH), 36.1 (⁴CH₂), 62.0 (O—¹CH₂); 83.0 (⁵C); 139.8 (N=CH), 169.8 (COO).

5.2.8.5. *trans*-4,5-EEMPO. ¹H NMR: 0.93 (d, 3H, ^{4b}CH₃), 1.31 (t, 3H, ²CH₃), 1.34–1.45 (m, 1H, ^{4a}CH_{2A}), 1.55–1.66 (m, 1H, ^{4a}CH_{2B}), 1.61 (s, 3H, ^{5a}CH₃), 2.30–2.48 (m, 1H, ³CH_{2B}), 2.72–2.81 (m, 1H, ⁴CH), 2.83–2.94 (m, 1H, ³CH_{2A}), 4.27 (m, 2H, ¹CH₂), 7.05 (t, 1H, ³J = 2.3 Hz, ²CH). ¹³C NMR: 11.6 (^{4b}CH₃), 13.9 (²CH₃), 14.8 (^{5a}CH₃), 22.7 (^{4a}CH₂), 32.7 (³CH₂), 44.2 (⁴CH), 62.3 (O—¹CH₂); 82.1 (⁵C); 136.1 (N=CH), 170.0 (COO).

5.2.8.6. *cis*-4,5-EEMPO. ¹H NMR: 0.97 (d, 3H, ^{4b}CH₃), 1.31 (t, 3H, ²CH₃), 1.34–1.45 (m, 1H, ^{4a}CH_{2A}), 1.55–1.66 (m, 1H, ^{4a}CH_{2B}), 1.70 (s, 3H, ^{5a}CH₃), 2.22–2.27 (m, 1H, ⁴CH), 2.32–2.43 (m, 1H, ³CH_{2B}), 2.80–2.90 (m, 1H, ³CH_{2A}), 4.27 (m, 2H, ¹CH₂), 7.22 (t, 1H, ³J = 2.6 Hz, ²CH). ¹³C NMR: 11.9 (^{4b}CH₃), 14.1 (²CH₃), 20.5 (^{5a}CH₃), 23.3 (^{4a}CH₂), 32.4 (³CH₂), 47.8 (⁴CH), 62.1 (O—¹CH₂); 81.9 (⁵C); 138.3 (N=CH), 168.1 (COO).

5.2.8.7. *trans*-5,4-EEMPO. ¹H NMR: 1.02 (d, 3H, ^{5b}CH₃), 1.18 (d, 3H, ^{4a}CH₃), 1.31 (t, 3H, ²bCH₃), 1.91–2.11 (m, 1H, ^{5a}CH_{2A}), 2.13–2.28 (m, 1H, ^{5a}CH_{2B}), 2.32 (m, 1H, ³CH_{2B}), 2.91 (m, 1H, ³CH_{2A}), 2.96 (m, 1H, ⁴CH), 4.27 (m, 2H, ¹CH₂), 7.10 (t, 1H, ³J = 2.3 Hz, ²CH). ¹³C NMR: 8.6 (^{5b}CH₃), 13.9 (²CH₃), 14.3 (^{4a}CH₃), 22.6 (^{5a}CH₂), 35.1 (³CH₂), 37.0 (⁴CH), 61.9 (O—¹CH₂); 84.8 (⁵C); 136.0 (N=CH), 169.7 (COO).

5.2.8.8. *cis*-5,4-EEMPO. 0.98 (d, 3H, ^{5b}CH₃), 1.09 (d, 3H, ^{4a}CH₃), 1.31 (t, 3H, ²bCH₃), 1.91–2.11 (m, 1H, ^{5a}CH_{2A}), 2.13–2.28 (m, 1H, ^{5a}CH_{2B}), 2.41 (m, 1H, ³CH_{2B}), 2.73 (m, 1H, ⁴CH), 2.81 (m, 1H, ³CH_{2A}), 4.27 (m, 2H, ¹CH₂), 7.18 (t, 1H, ³J = 2.3 Hz, ²CH). ¹³C NMR: 7.0 (^{5b}CH₃), 14.0 (²CH₃), 15.2 (^{4a}CH₃), 23.7 (^{5a}CH₂), 34.21 (³CH₂), 34.25 (⁴CH), 61.8 (O—¹CH₂); 85.4 (⁵C); 138.0 (N=CH), 168.2 (COO).

5.2.9. Preparation of lipid hydroperoxides. Linoleic acid hydroperoxide was synthesized according to O'Brien.²⁴

Briefly, linoleic acid was air-oxidized for 72 h in the dark at room temperature. The oxidation mixture was dissolved in petroleum ether (boiling range 60–90 °C) and extracted four times with water/methanol (v/v = 1:3). The obtained methanolic phase was counter-extracted four times with petroleum ether (boiling range 60–90 °C) and evaporated under reduced pressure. The obtained hydroperoxide was dissolved in ethanol and stored in liquid nitrogen. The concentration of hydroperoxide was determined by UV spectroscopy based on an extinction coefficient of $\epsilon_{233\text{nm}} = 25250 \text{ M}^{-1} \text{ cm}^{-1}$ in ethanol.²⁴

5.3. Instruments

UV–vis spectra were recorded between 200 and 350 nm on Hitachi 150–20 and U-3300 spectrophotometers in double-beam mode. IR spectra were recorded as film on an ATI Mattson Genesis Series FTIR spectrometer (see also Table 2).

For EPR experiments, Bruker spectrometers (ESP300E and EMX) were used, operating at 9.7 GHz with 100 kHz modulation frequency, equipped with a rectangular TE₁₀₂ or a TM₁₁₀ microwave cavity.

NMR spectra were recorded on a Bruker Avance at 300.13 MHz for ¹H, and 75.47 MHz for ¹³C. CDCl₃ was used as the solvent throughout, TMS (tetramethylsilane) as the internal standard. ¹³C peaks were assigned by means of APT (attached proton test), HMQC (¹H-detected heteronuclear multiple-quantum coherence), and HMBC (heteronuclear multiple bond connectivity) spectra. All chemical shift data are given in ppm units, coupling constants in Hz.

Mass spectra were obtained as follows: samples were diluted in the ratio 1:10.000 in 70% methanol containing 0.1% formic acid and injected offline to ESI Q-TOF MS on a Waters Micromass Q-TOF Ultima Global at a flow rate of 5 µl/min. To acquire appropriate spectra for every sample, capillary voltage was adjusted between 1.2 and 3.0 kV. The mass spectrometer had been previously tuned with [Glu1]-fibrinopeptide B to give highest possible sensitivity and a resolution of 10.000 (FWHM). Mass tuning of the TOF analyzer was done in the tandem MS mode using again [Glu1]-fibrinopeptide B. Data analysis were performed with MassLynx 4.0 SP4 Software (Waters Micromass).

Acknowledgment

The authors wish to thank P. Jodl for skilful technical assistance in synthesis, purification, and characterization of the spin traps.

References and notes

1. Stolze, K.; Udilova, N.; Rosenau, T.; Hofinger, A.; Nohl, H. *Biochem. Pharmacol.* **2005**, *69*, 297.
2. Stolze, K.; Rohr-Udilova, N.; Rosenau, T.; Stadtmüller, R.; Nohl, H. *Biochem. Pharmacol.* **2005**, *69*, 1351.
3. Stolze, K.; Rohr-Udilova, N.; Rosenau, T.; Hofinger, A.; Kolarich, D.; Nohl, H. *Bioorg. Med. Chem.* **2006**, *14*, 3368.
4. Tsai, P.; Ichikawa, K.; Mailer, C.; Pou, S.; Halpern, H. J.; Robinson, B. H.; Nielsen, R.; Rosen, G. M. *J. Org. Chem.* **2003**, *68*, 7811.
5. Tsai, P.; Marra, J. M.; Pou, S.; Bowman, M. K.; Rosen, G. M. *J. Org. Chem.* **2005**, *70*, 7093.
6. Roubaud, V.; Lauricella, R.; Bouteiller, J. C.; Tuccio, B. *Arch. Biochem. Biophys.* **2002**, *397*, 51.
7. Dikalov, S. I.; Mason, R. P. *Free Radical Biol. Med.* **2001**, *30*, 187.
8. Stolze, K.; Udilova, N.; Nohl, H. *Free Radical Biol. Med.* **2000**, *29*, 1005.
9. Stolze, K.; Udilova, N.; Nohl, H. *Biol. Chem.* **2002**, *383*, 813.
10. Stolze, K.; Udilova, N.; Nohl, H. *Biochem. Pharmacol.* **2002**, *63*, 1465.
11. Stolze, K.; Udilova, N.; Rosenau, T.; Hofinger, A.; Nohl, H. *Biol. Chem.* **2003**, *384*, 493.
12. Stolze, K.; Udilova, N.; Nohl, H. *Acta Biochim. Pol.* **2000**, *47*, 923.
13. Clément, J.-L.; Ferré, N.; Siri, D.; Karoui, H.; Rockenbauer, A.; Tordo, P. *J. Org. Chem.* **2005**, *70*, 1198.
14. Rota, C.; Barr, D. P.; Martin, M. V.; Guengerich, F. P.; Tomasi, A.; Mason, R. P. *Biochem. J.* **1997**, *328*, 565.
15. Van der Zee, J.; Barr, D. P.; Mason, R. P. *Free Radical Biol. Med.* **1996**, *20*, 199.
16. Akaike, T.; Sato, K.; Ijiri, S.; Miyamoto, Y.; Kohno, M.; Ando, M.; Maeda, H. *Arch. Biochem. Biophys.* **1992**, *294*, 55.
17. Kalyanaraman, B.; Mottley, C.; Mason, R. P. *J. Biol. Chem.* **1983**, *258*, 3855.
18. Chamulitrat, W.; Takahashi, N.; Mason, R. P. *J. Biol. Chem.* **1989**, *264*, 7889.
19. Davies, M. J. *Biochim. Biophys. Acta* **1988**, *964*, 28.
20. Davies, M. J. *Biochem. J.* **1989**, *257*, 603.
21. Olive, G.; Mercier, A.; LeMoigne, F.; Rockenbauer, A.; Tordo, P. *Free Radical Biol. Med.* **2000**, *28*, 403.
22. Zhang, H.; Joseph, J.; Vasquez-Vivar, J.; Karoui, H.; Nsanzumuhire, C.; Martásek, P.; Tordo, P.; Kalyanaraman, B. *FEBS Lett.* **2000**, *473*, 58.
23. Zhao, H.; Joseph, J.; Zhang, H.; Karoui, H.; Kalyanaraman, B. *Free Radical Biol. Med.* **2001**, *31*, 599.
24. O'Brien, P. J. *Can. J. Biochem.* **1969**, *47*, 485.